

Mapping City Lights With Nighttime Data from the DMSP Operational Linescan System

Christopher D. Elvidge, Kimberly E. Baugh, Eric A. Kihn, Herbert W. Kroehl, and Ethan R. Davis

Abstract

The Defense Meteorological Satellite Program (DMSP) Operational Linescan System (OLS) has a unique capability to detect low levels of visible and near-infrared (VNIR) radiance at night. With the OLS "VIS" band data, it is possible to detect clouds illuminated by moonlight, plus lights from cities, towns, industrial sites, gas flares, and ephemeral events such as fires and lightning illuminated clouds. This paper presents methods which have been developed for detecting and geolocating VNIR emission sources with nighttime DMSP-OLS data and the analysis of image time series to identify spatially stable emissions from cities, towns, and industrial sites. Results are presented for the United States.

Introduction

The distribution of human populations across the Earth's surface has been identified as one of the key datasets required for improved understanding of human impacts on land and water resources, as well as for improved modeling of the environmental consequences which may be expected under varying models of economic growth (Clarke and Rhind, 1992). Census data can provide population numbers based on administrative units such as state, county, city, or town, but do not provide spatially explicit detail on the outlines of populated places. There are global map datasets, such as the Defense Mapping Agency (DMA) Operational Navigation Charts (ONC); however, these products are typically a decade or more out of date. The populated place lines (PPL) that show the outline of urban areas, available in the DMA Digital Chart of the World (DCW), were digitized from the ONC charts, thus propagating out-of-date data into "new" digital maps.

Satellite sensors capable of acquiring frequent global coverage would seem to have the potential for producing and updating global maps of city and town locations. Unfortunately, urban areas, villages, and towns are difficult to identify with coarse resolution satellite data from the NOAA Advanced Very High Resolution Radiometer (AVHRR) due to a lack diagnostic spectral features. While spatial features such as road networks and many buildings can be identified

C.D. Elvidge is with the Desert Research Institute, University of Nevada System, Reno, NV 89506 and the Solar-Terrestrial Physics Division, National Oceanic and Atmospheric Administration, National Geophysical Data Center, 325 Broadway, Boulder, CO 80303 (cde@ngdc.noaa.gov).

E.A. Kihn and H.W. Kroehl are with the Solar-Terrestrial Physics Division, National Oceanic and Atmospheric Administration, National Geophysical Data Center, 325 Broadway, Boulder, CO 80303.

K.E. Baugh and E.R. Davis are with the Cooperative Institute for Research in Environmental Sciences, University of Colorado, Boulder, CO 80303.

using high spatial resolution data produced by the Landsat, SPOT, and other satellites, the prospects for generating and updating a global map showing where people are concentrated is daunting, even from a data acquisition standpoint.

Since the 1970s, the U.S. Air Force Defense Meteorological Satellite Program (DMSP) has operated satellite sensors capable of detecting the visible and near-infrared (VNIR) emissions from cities and towns. The DMSP Operational Linescan System (OLS) acquires global daytime and nighttime imagery of the Earth in two spectral bands (VIS and TIR). The nighttime "VIS" bandpass straddles the VNIR portion of the spectrum (0.5 to 0.9 μm). The VIS band signal is intensified at night using a photomultiplier tube (PMT), making it possible to detect faint VNIR emission sources. The PMT system was implemented for the detection of clouds at night. An unanticipated consequence of the nighttime light intensification is the detection of city lights, gas flares, and fires. Figure 1 shows city lights in Europe from 6 January 1995.

The potential use of nighttime OLS data for the observation of city lights and other VNIR emission sources was first noted in the 1970s by Croft (1973, 1978, 1979). However, during the first 20 years of the DMSP no digital archive was maintained and only film strips were available to the scientific community. Sullivan (1989) produced a 10-km resolution global image of OLS observed VNIR emission sources using film strip archived at the National Snow and Ice Data Center. In 1992 DoD and NOAA established a digital archive for the DMSP program at the NOAA National Geophysical Data Center.

Recent results obtained with the digital DMSP-OLS data suggest that a global map of city lights could be readily produced and updated. During the past year the authors have developed algorithms to identify and geolocate VNIR emission sources in nighttime OLS imagery. Time series analysis is then used to distinguish stable VNIR emissions generated by villages, towns, and cities from ephemeral VNIR emissions arising from fires. This paper describes the unique characteristics of the OLS which make it possible to observe faint sources of VNIR emission and outlines the procedures which have been developed to construct maps of stable VNIR emission sources.

The DMSP Operational Linescan System

The Operational Linescan System (OLS) is an oscillating scan radiometer designed for cloud imaging with two spectral bands (VIS and TIR) and with a swath of ~ 3000 km. The "VIS" bandpass straddles the visible and near-infrared (VNIR) portion of the spectrum. The wide swath widths provide for

Photogrammetric Engineering & Remote Sensing,
Vol. 63, No. 6, June 1997, pp. 727-734.

0099-1112/97/6306-727\$3.00/0

© 1997 American Society for Photogrammetry
and Remote Sensing



Figure 1. City lights of Europe observed with the DMSP-OLS on 6 January 1995.

global coverage four times a day: dawn, day, dusk, and night. DMSP platforms are stabilized using four gyroscopes (three-axis stabilization), and platform orientation is adjusted using a star mapper, an Earth limb sensor, and a solar detector.

The low-light sensing capabilities of the OLS at night permit the measurement of radiances in the VIS band down to 10^{-9} watts/cm²/sr/μm. This is greater than four orders of magnitude more sensitive (see Figure 2) than the OLS daytime VIS band or the VNIR bands of other sensors, such as the NOAA AVHRR, Landsat Thematic Mapper, or NASA's Airborne Visible / Infrared Imaging Spectrometer (AVIRIS). The VIS band PMT system was implemented to facilitate the detection of clouds at night using moonlight. With sunlight eliminated, the light intensification results in a unique data set in which city lights, gas flares, lightning illuminated clouds, and fires can be observed.

The VIS band gains are computed onboard based on scene source illumination predicted from solar elevation and lunar phase and elevation. The base gain is modified every 0.4 milliseconds by an on-board along-scan gain algorithm. In addition, a BRDF (bidirectional reflectance distribution function) algorithm further adjusts the gain in the scan segment where the illumination angle approaches the observation angle, resulting in enhanced specular reflectance. The objective of the two types of along-scan gain changes is to

produce visually consistent imagery of clouds at all scan angles for use by Air Force meteorologists. During the darkest 12 nights of the lunar cycle, illumination is too low to detect

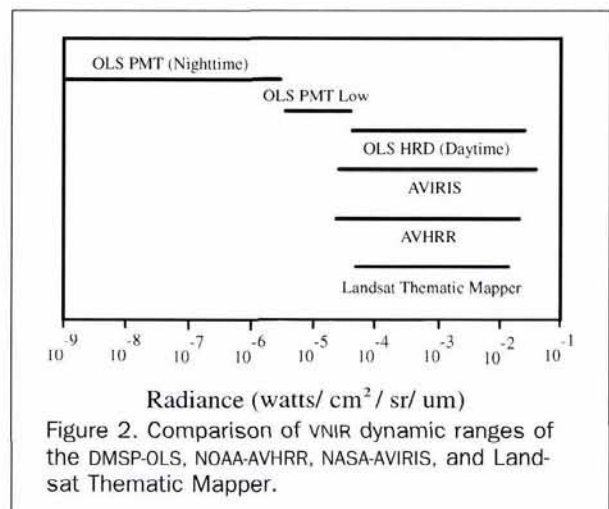


Figure 2. Comparison of VNIR dynamic ranges of the DMSP-OLS, NOAA-AVHRR, NASA-AVIRIS, and Landsat Thematic Mapper.

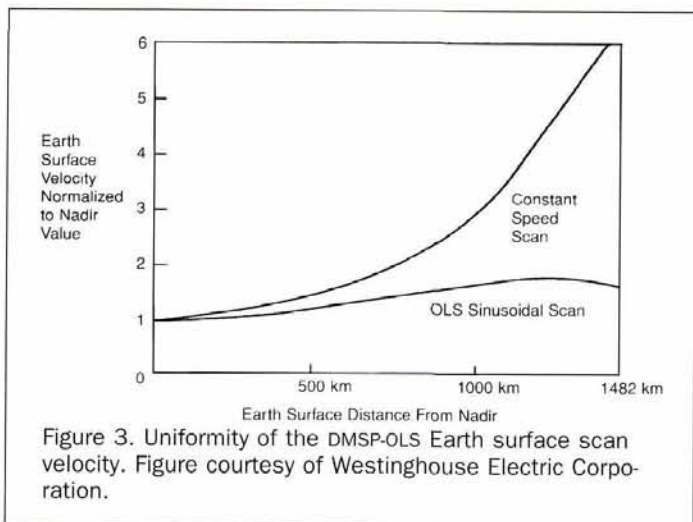


Figure 3. Uniformity of the DMSP-OLS Earth surface scan velocity. Figure courtesy of Westinghouse Electric Corporation.

clouds in the VIS band. Under these conditions, the effects of the along-scan gain and BRDF algorithms are minimized and the gain rises to its maximum monthly level.

There are two spatial resolution modes in which data can be acquired. The full resolution data, having a nominal spatial resolution of 0.56 km, is referred to as "fine." On-board averaging of five by five blocks of fine data produces "smooth" data with a nominal spatial resolution of 2.8 km. Most of the data received by NOAA-NGDC is in the smooth spatial resolution mode.

The OLS uses several methods to constrain the enlargement of pixel dimensions which normally occur as a result of cross-track scanning (Lieske, 1981). The OLS features a sinusoidal scan motion, which maintains a nearly constant along-track pixel-to-pixel ground sampling distance (GSD) of 0.56 km at all scan angles in the fine resolution data (Figure 3). The along-scan GSD for fine resolution data starts at 0.31 km at nadir and slowly rises to 0.55 km at 1200 km surface distance from nadir, decreasing again to 0.5 km by the end of scan. The detector image rotates as a function of the scan angle, and the shape, size, and orientation of the OLS detectors was designed to take advantage of this rotation to reduce the expansion of the EIFOV (effective instantaneous field of view) at off-nadir scan angles. In addition, the PMT electron aperture is magnetically switched (deflected) during the outer quarter of each scan (Figure 4), again reducing the size of the detector image on the ground surface. The along-scan changes in the projection of the detector image on the Earth's surface are illustrated in Figure 5. The EIFOV of the nighttime VIS band fine resolution data starts at 2.2 km at the nadir and expands to 4.3 km at 766 km out from the nadir. After the aperture is switched, the IFOV is reduced to 3.0 km and expands to 5.4 km at the far edges of the scan. Thus, the EIFOV is substantially larger than the GSD in both the along-track and along-scan directions.

Production of a City Lights Dataset of the United States

In order to develop procedures suitable for producing a global map of VNIR emission sources, we have produced a "city lights" dataset for the United States using smooth resolution OLS data. The procedures involve the detection and geolocation of VNIR emission sources and clouds from a large number of nighttime OLS orbital images, their mapping to a consistent reference grid, and the use of image time series analysis to distinguish stable lights produced by cities, towns, and industrial facilities from ephemeral lights arising from fires and lightning. The time series approach is re-

quired in order to ensure that each land area has been covered with sufficient cloud-free observations to determine the presence or absence of spatially stable VNIR emission. Heavy cloud cover blocks the detection of VNIR emission sources and light cloud cover tends to diffuse lights present on the Earth's surface, making them appear larger than their actual size.

Development of a spatially coherent image time series requires the use of a reference grid with finer spatial resolution than the input imagery. We have used the one-kilometre grid developed for the NASA-USGS Global 1-km AVHRR project (Eidenshink and Faundeen, 1994) interrupted Goode Homologous Projection (Goode, 1925; Steinwand, 1994). This projection is optimized to provide a uniform grid cell size at all latitudes and contiguous land masses (except Antarctica). These are favorable characteristics for the production of global land datasets from raster imagery (Steinwand, 1994). Once an image time series is assembled, it is then possible to analyze the data to discriminate between stable VNIR emission sources (cities, towns, industrial sites) and ephemeral VNIR emissions from phenomena such as fires.

Geolocation

Our geolocation algorithm operates in the forward mode, projecting the center point of each pixel onto the Earth's surface. The geolocation algorithm estimates the latitude and longitude of pixel centers based on the geodetic subtrack of the satellite orbit, satellite altitude, OLS scan angle equations, an Earth sea level model, and digital terrain data. The geodetic subtrack of each orbit is modeled using daily radar bevel vector sightings of the satellite (provided by Naval Space Command) as input into an Air Force orbital mechanics model that calculates the satellite position every 0.4208 seconds. The satellite heading is estimated by computing the tangent to the orbital subtrack. We have used an oblate ellipsoid model of sea level and have used Terrain Base (Row and Hastings, 1995) as a source of digital terrain elevations.

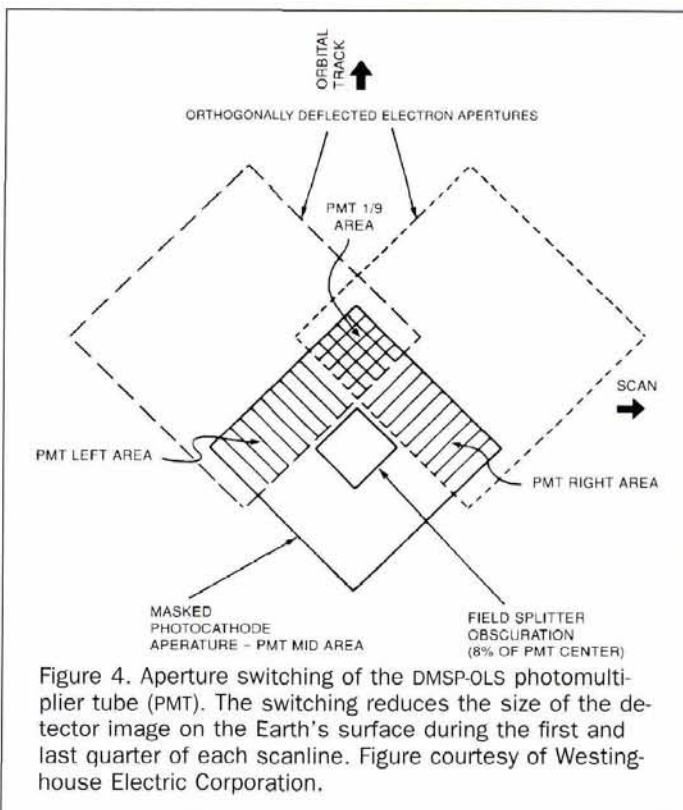


Figure 4. Aperture switching of the DMSP-OLS photomultiplier tube (PMT). The switching reduces the size of the detector image on the Earth's surface during the first and last quarter of each scanline. Figure courtesy of Westinghouse Electric Corporation.

Reference Grid

A 3000-line by 5000-sample reference grid of 1-km pixels was extracted from the global reference grid established for the 1-km AVHRR project (Eidenshink and Faundeen, 1995). Our reference grid begins with line 3000, sample 6700 of the larger global grid. To fill geolocated OLS data into the reference grid, we find the grid cell closest to the latitude and longitude of the OLS pixel center and fill in the surrounding three by three block of pixels.

Image Selection and Suborbiting

Data from a total of 236 smooth resolution OLS orbits covering the United States were selected from the DMSP archive from October 1994 through March of 1995. Fifty orbits were from the F-10 satellite and 186 orbits came from the F-12 satellite. The October to March time period was selected based on the completeness of the archive during this time period and also to avoid solar illumination which would be present in the northern portions of the area during period surrounding the summer solstice. Orbits were selected from nights having less than half moon. Data volume was further reduced by subsetting the orbits to retain only image data covering the area from 20 to 55 degrees north latitude.

Removal of Glare

One adverse effect of the PMT light intensification is that the OLS is quite sensitive to scattered sunlight. Under certain geometric conditions, portions of the OLS are illuminated by sunlight and scattered sunlight enters the optically black tunnel in which the OLS telescope is housed. The result is saturated visible band data covering large portions of the imagery, a condition referred to as glare. The exact shape and orbital position of the glare changes through the year. Glare was encountered for a small number of the orbits used, primarily in the northwest portion of the United States.

An automated algorithm has been developed to detect and remove glare from OLS images. Glare is detected when a 40 by 40 block of pixels is encountered with all pixels having saturated digital number (DN) counts of 63. The detection of the saturated block of pixels initiates an expanding search for all adjacent pixels with DN counts of 40 or greater. The DN counts for these pixels are set to zero. The cell size of 40 by 40 for glare detection was selected to avoid mistaking large cities as glare and to accommodate variations in glare size and shape.

Tracking of Orbital Coverages

The number of OLS data coverages for each of the 1-km cells in the reference grid was determined by geolocating the outer perimeters of non-zero data from each orbit (missing data have values of zero) and projecting the outlines into the reference grid. Areas inside the polygons were assigned values of 1. The total number of coverages for each grid cell was then determined by adding the values of all the coverage polygons in the time series. During this process it was determined that five of the 236 orbits drawn from the archive contained no data between 20 and 55 degrees north latitude, thus reducing the number of orbits containing usable data to 231. Total number of coverages over the land areas of the reference grid ranged from 50 to 120 (Figure 6). The highest numbers of coverages occur in the northern part of the reference grid. Many of the satellite F-10 orbits lacked data in the southern portion of the grid. In addition, there is greater overlap between orbits in the northern part of the reference grid.

Cloud Screening

Because of the low level of lunar illumination present in the orbital segment, it was not possible to use the VIS band to

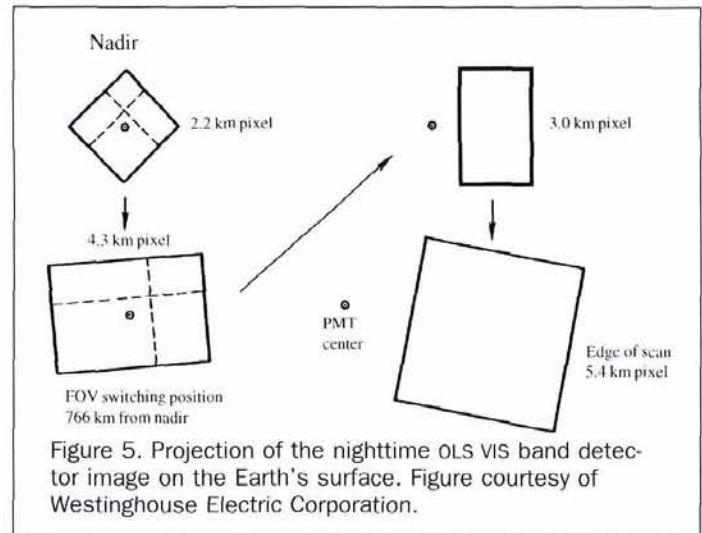
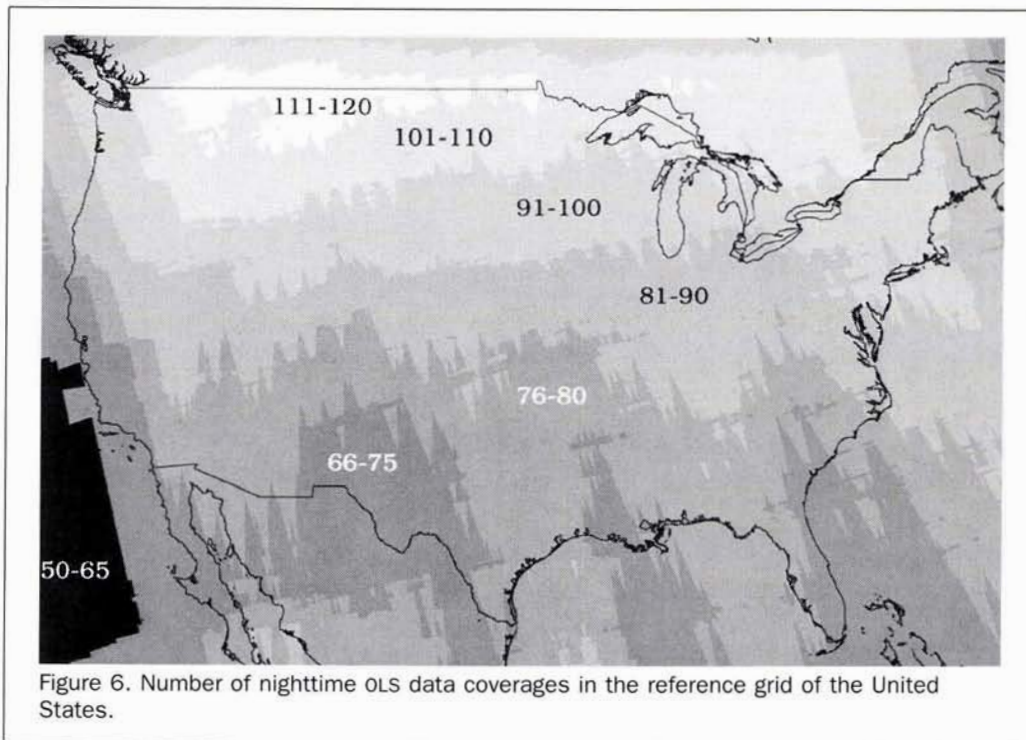


Figure 5. Projection of the nighttime OLS VIS band detector image on the Earth's surface. Figure courtesy of Westinghouse Electric Corporation.

screen for clouds. The cloud screening was based entirely on thresholds set on the TIR band. Clouds are generally colder than the Earth's surface. However, the separation of cloud pixels from Earth surface pixels using TIR thresholding is complicated by seasonal, latitudinal, and altitudinal variations in the background Earth surface temperature. The separation of clouds from Earth surface pixels is relatively easy at low latitudes where there is generally a large temperature difference between pixels of cloud tops and pixels containing land or ocean. Because of the strong latitudinal effects on the TIR threshold for cloud screening in our data, we segmented each of the 231 orbital sections into five latitudinal bands, and we visually selected a TIR threshold for discriminating the cloud pixels (Figure 7). Cloud pixels in each orbit were then geolocated and projected into a reference grid set up to serve as a counter, with grid cells values increasing by one for each orbit in which a cloud was present. Then the total number of "cloud-free" observations in the reference grid was determined by subtracting the cloud counts from the coverage counts (Figure 8). Most land areas in the reference grid had 46 to 100 cloud-free observations. Those areas that had less than 46 "cloud-free" observations were generally located in high elevation areas in the western third of the grid, where snow pack was probably misidentified as cloud cover in the OLS TIR band data. The lowest number of "cloud-free" observations (19) occurred in the Sierra Nevada of California. Areas having the highest numbers of cloud-free observations are in the northern part of the reference grid, reflecting the fact that these areas have the largest numbers of observations (Figure 6).

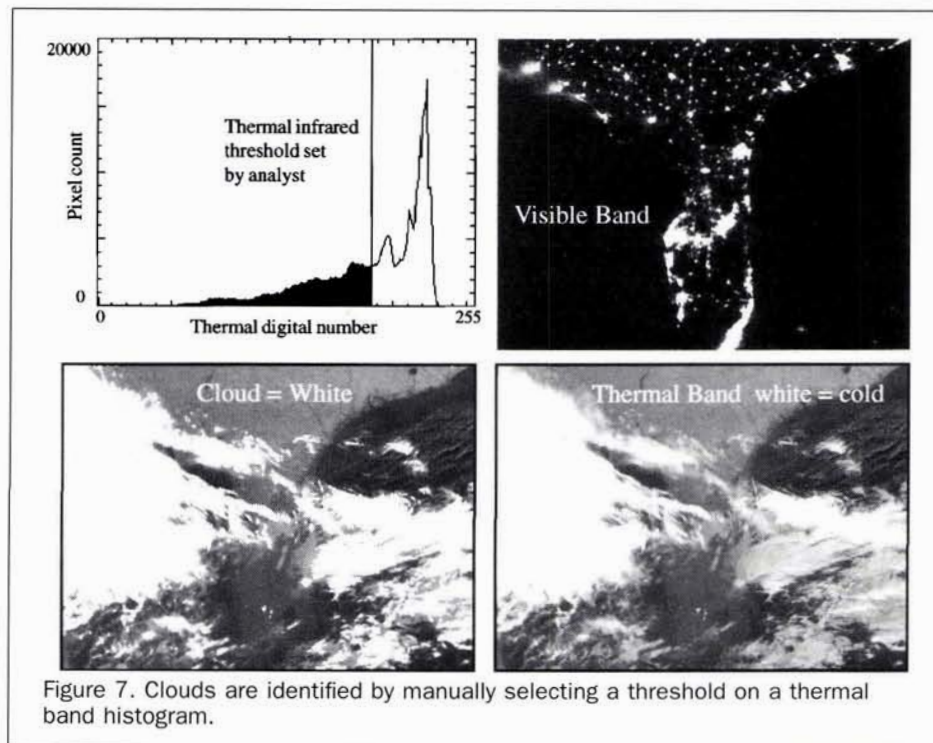
Identification of VNIR Emission Sources

Because of brightness variations which occur within and between orbits, it is not possible to set a single digital number (DN) threshold for identifying VNIR emission sources. We have developed an algorithm for automatic detection of VNIR emission sources (lights) in nighttime OLS data using thresholds established based on the local background. Lights are picked in 20- by 20-pixel blocks, with the local background being drawn from the surrounding 50- by 50-pixel block. This "light picking" algorithm excludes bright pixels in the selection of a background pixel set, which is then analyzed to establish a brightness threshold for the detection of VNIR emission sources. The resulting threshold is applied to the central 20- by 20-pixel block inside the 50- by 50-pixel block (Figure 9). Processing of an image proceeds by tiling the results from adjacent 20- by 20-pixel blocks.



The nested configuration of the 20 by 20 block inside of the 50 by 50 block was designed to provide rapid processing of suborbits and to accommodate changes in background brightness. Identifying the local threshold for a 20 by 20 block is 400 times faster than processing a new threshold for each individual pixel. There is 60 percent overlap between the 50- by 50-pixel outer block used to generate background statistics. This results in smooth transitions in threshold levels, minimizing threshold disparities between adjacent 20- by 20-pixel blocks.

The distribution of DN values in each 50- by 50-pixel cell is analyzed to identify the set of pixels for use as the local background. VIS band DN values range from 0 to 63. Zeros are missing data and 63s are saturated pixels. The lower limit of the background is taken to be DN = 1. The upper limit of the background is determined using a frequency distribution of pixel counts versus DN values. Starting from DN = 63 and working down, the frequency distribution is analyzed to detect the first DN value where five consecutive DN bins have greater than 0.4 percent of the total pixel counts.



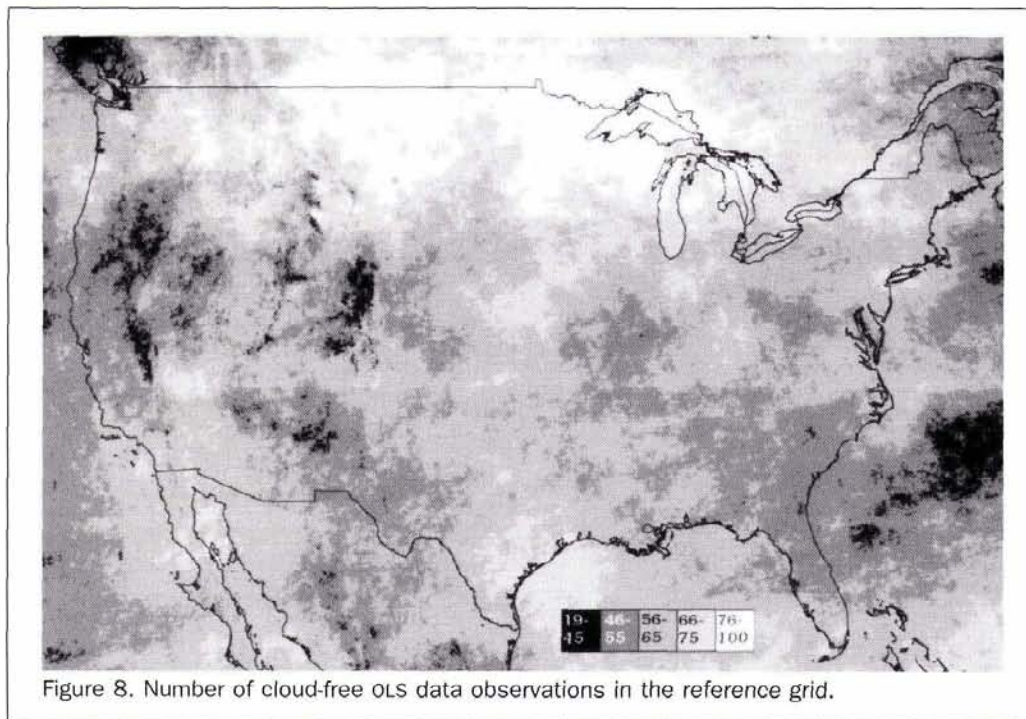


Figure 8. Number of cloud-free OLS data observations in the reference grid.

For a full 50 by 50 cell, this corresponds to a search threshold of 10 pixels per DN bin. Once the upper limit of the background is selected, the mean and standard deviation of the background pixel set is calculated. Pixels containing VIS band emission sources are then identified using a threshold set at the DN value of the background mean plus four standard deviations. Figure 9 shows an example of the light picker applied to Myrtle Beach, South Carolina.

Identification of Stable Lights

After the VNIR emission sources and clouds have been identified, the pixels containing cloud-free VNIR emission sources

are geolocated and placed into the reference grid. One reference grid plane is generated for each orbit. A counter is then run through the time series to determine the number of times a cloud-free light was detected in each grid cell. This value is then divided by the total number of cloud-free observations (Figure 8) and multiplied by 100. This yields the percent frequency with which a VNIR emission was detected in each grid cell based solely on cloud-free OLS observations.

Results

The results of our processing methodology are shown in Figure 10, an image of the reference grid showing the fre-

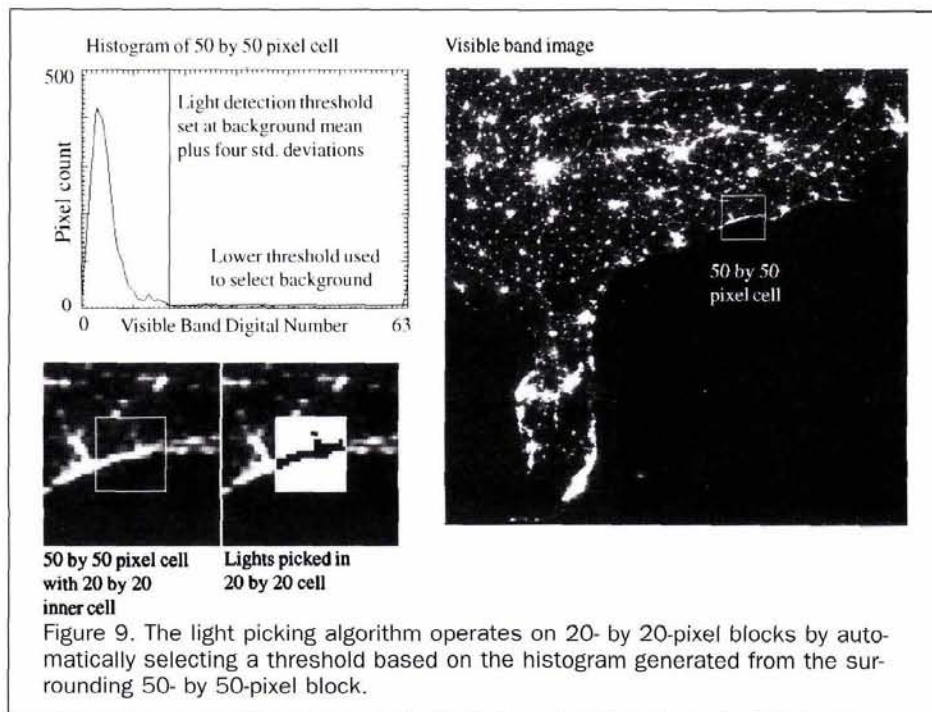


Figure 9. The light picking algorithm operates on 20- by 20-pixel blocks by automatically selecting a threshold based on the histogram generated from the surrounding 50- by 50-pixel block.



Figure 10. City lights of the United States, displayed by showing all reference grid positions which had VNIR emissions in at least 10 percent of the cloud-free observations as white.

quency with which cloud-free lights were detected in each grid cell, relative to the total number of cloud-free observations (Figure 8). The majority of the detected features are lights from cities and towns. A set of oil platforms can be observed in the Gulf of Mexico south of Louisiana. An as yet indeterminate number of the features identified on the land are from isolated industrial, oil and gas production, and mining sites.

Examination of cross sections through the city light features in Figure 10 indicate that there is typically a central area with a high number of light observations and that the frequency of light observations rapidly declines at the edges of features. Several examples of this phenomena are shown in the cross section at the bottom of Figure 11. We believe that this phenomena is due to errors in the geolocation of the lights, subpixel detection of lights, and diffusion of lights below undetected fog and thin cloud cover. The OLS TIR band has limited capability to detect warm clouds, such as fog.

Figure 11 shows the stable lights identified for the Washington, D.C. area, with coastlines, state boundaries, major roads, and populated place lines (PPL) from the Digital Chart of the World (DCW). The OLS identified stable lights for nearly all of the DCW populated place lines. However, the OLS stable lights cover larger areas than the DCW-PPL. This is not surprising given that the DCW-PPL were digitized from a map produced in 1970 and do not include the amount of urban / suburban growth which has occurred during the 25 years which have elapsed.

Conclusion

The Defense Meteorological Program (DMSP) Operational Line-scan System (OLS) has a unique capability to detect visible and near-infrared (VNIR) emission sources at night, down to radiances of 10^{-9} watts/cm²/sr/μm. This is more than four orders of magnitude fainter than the minimal detectable VNIR radiances from satellite sensors optimized for daytime observation of reflected solar irradiance.

It has been known since the 1970s that lights from cities, towns, industrial sites, and gas flares were detectable with nighttime data from the DMSP-OLS. In the 1980s several regional to global scale maps of VNIR emission sources were produced using analog data (film). We present the first method for mapping city lights using digital data from the OLS.

The digital method for mapping city lights with DMSP-OLS data employs data from a large numbers of orbits, use of a local background in the detection of VNIR emission sources, and screening for cloud cover. Clouds can either obscure or diffuse the VNIR light emitted from the Earth's surface. Thus, the tracking of cloud cover is crucial to ensure that sufficient cloud-free observations have been made in each land area and to exclude lights diffused by clouds. These procedures make it possible to develop a statistical profile of the frequency with which individual features can be detected and to delineate lights from small towns which may not be detectable every night, even under cloud-free conditions. Many cities were detected in 90 to 100 percent of the cloud-free observations. However, smaller towns were detected with less frequency, in some cases only 10 to 20 percent of the time.

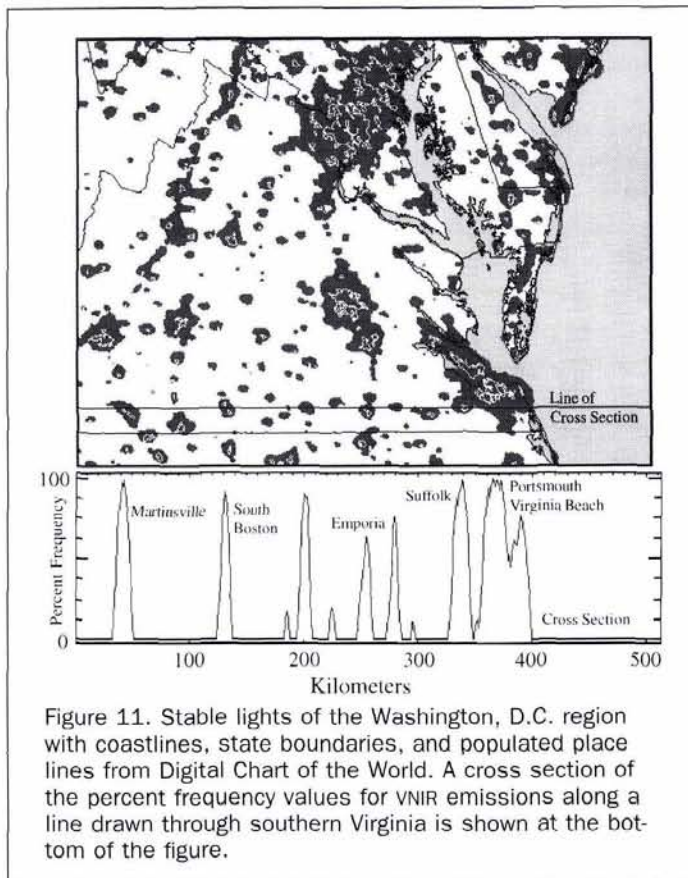


Figure 11. Stable lights of the Washington, D.C. region with coastlines, state boundaries, and populated place lines from Digital Chart of the World. A cross section of the percent frequency values for VNIR emissions along a line drawn through southern Virginia is shown at the bottom of the figure.

In addition to a geolocation accuracy assessment, the authors are investigating the potential for reducing the edge effects on the outlines of the stable lights. We believe that a substantial sharpening of the features could be accomplished by only retaining the pixels occurring in the upper portions of the individual percent frequency peaks. The edge effect can be observed in the cross section at the bottom of Figure 11. Because of the wide range in values for the percent frequency peaks, it is not possible to take a single threshold value for sharpening the features. For example, if a constant threshold of 30 percent were applied, minimal sharpening would occur for feature which were present 95 percent of the time, and features which were present 20 percent of the time, such as smaller towns and villages, would be lost.

Recent discussions with engineers in charge of operating the OLS indicate that it is feasible to calibrate the nighttime OLS data to radiance units based on the pre-flight sensor calibration. We are now implementing the along-scan gain control and BRDF algorithms required to retrieve radiances from nighttime OLS data.

Over the next year we expect to complete a global map of stable VNIR emission sources which will be available to the scientific community for the analysis of social, environmental, and energy issues. By combining the map of stable

lights with observations from single nights, it will be possible to detect blackouts and brownouts in the electrical grid resulting from either natural or human events. In the longer term, we expect it will be possible to periodically update the global city light map to detect the expansion of urban areas. The DMSP program is expected to continue to operate OLS sensors continuously until the later part of the next decade and perhaps until the year 2010. The planned NOAA-Department of Defense converged system of meteorological sensors will preserve the low light sensing capability initiated with the OLS. Thus, the mapping of stable VNIR emission sources using nighttime satellite data can be expected to be a continuing source of information for the coming decades.

Acknowledgments

This research was supported in part by the DoD Strategic Environmental Research and Development Program (SERDP). Figures 3, 4, and 5 were provided to the authors by Roger Lieske of Westinghouse Electric Corporation. The DMSP data collection for this research was provided by the DMSP program office, which also provided support for the archive at NOAA-NGDC. The authors appreciate the cooperation of the U.S. Air Force Global Weather Central for providing NOAA-NGDC with DMSP data for the DMSP archive.

References

- Clarke, J.T., and D.W. Rhind (editors), 1992. *Population Data and Global Environmental Change*, International Social Science Council, Human Dimensions of Global Environmental Change Programme, Report No. 3, Paris.
 - Croft, T.A., 1973. Burning waste gas in oil fields. *Nature*, 245:375-376.
 - , 1978. Nighttime images of the earth from space, *Scientific American*, 239:68-79.
 - , 1979. *The Brightness of Lights on Earth at Night, Digitally Recorded by DMSP Satellite*, Stanford Research Institute Final Report Prepared for the U.S. Geological Survey.
 - Eidenshink, J.C., and J.L. Faundeen, 1994. The 1-km AVHRR global land data set: First stages in implementation, *International Journal of Remote Sensing*, 15:3443-3462.
 - Goode, J.P., 1925. The Homolosine projection: A new device for portraying the Earth's surface entire, *Association of American Geographers, Annals*, 115:119-125.
 - Lieske, R.W., 1981. DMSP primary sensor data acquisition, *Proceedings of the International Telemetry Conference*, 17:1013-1020.
 - Row, L.W., III, and D.A. Hastings, 1995. *TerrainBase Worldwide Digital Terrain Data, Documentation Manual and CD-ROM*, NOAA National Geophysical Data Center, Boulder, Colorado, NGDC Publication KGRD 30, 185 p.
 - Steinwand, D.R., 1994. Mapping raster imagery into the interrupted Goode Homolosine Projection, *International Journal of Remote Sensing*, 15:3463-3472.
 - Sullivan, W.T., III, 1989. A 10 km resolution image of the entire night-time Earth based on cloud-free satellite photographs in the 400-1100 nm band, *International Journal of Remote Sensing*, 10: 1-5.
- (Received 19 October 1995; accepted 13 February 1996; revised 18 April 1996)